01 Mar 2023

Incoherency in Central American Hydroclimate Proxy Records Spanning the Last Millennium

Jonathan Obrist-Farner
Missouri University of Science and Technology, obristj@mst.edu

Byron A. Steinman

Nathan D. Stansell

Jeremy Maurer
Missouri University of Science and Technology, jlmd9g@mst.edu

Recommended Citation

J. Obrist-Farner et al., "Incoherency in Central American Hydroclimate Proxy Records Spanning the Last Millennium," *Paleoceanography and Paleoclimatology*, vol. 38, no. 3, article no. e2022PA004445, American Geophysical Union; Wiley, Mar 2023.
The definitive version is available at https://doi.org/10.1029/2022PA004445

Paleoceanography and Paleoclimatology

AGU ADVANCING EARTH AND SPACE SCIENCE

RESEARCH ARTICLE
10.1029/2022PA004445

Key Points:

- We developed two precipitation proxy records from Central America
- We found distinct differences in hydroclimate between the two study sites during the last ~1,000 years
- Nine additional hydroclimate records suggest that hydroclimate in Central America has been highly variable across space and time

Supporting Information:

Supporting Information may be found in the online version of this article.

Correspondence to:

J. Obrist-Farner,
obristj@mst.edu

Citation:

Obrist-Farner, J., Steinman, B. A., Stansell, N. D., & Maurer, J. (2023). Incoherency in Central American hydroclimate proxy records spanning the last millennium. *Paleoceanography and Paleoclimatology*, *38*, e2022PA004445. https://doi.org/10.1029/2022PA004445

Received 14 MAR 2022
Accepted 21 FEB 2023

Incoherency in Central American Hydroclimate Proxy Records Spanning the Last Millennium

Jonathan Obrist-Farner[1], Byron A. Steinman[2], Nathan D. Stansell[3], and Jeremy Maurer[1]

[1]Geosciences and Geological and Petroleum Engineering Department, Missouri University of Science and Technology, Rolla, MO, USA, [2]Large Lakes Observatory and Department of Earth and Environmental Sciences, University of Minnesota Duluth, Duluth, MN, USA, [3]Department of Earth, Atmosphere, and Environment, Northern Illinois University, DeKalb, IL, USA

Abstract Continued global warming is expected to result in reduced precipitation and a drier climate in Central America. Projections of future changes are highly uncertain, however, due to the spatial resolution limitations of models and insufficient observational data coverage across space and time. Paleoclimate proxy data are therefore critical for understanding regional climate responses during times of global climate reorganization. Here we present two lake-sediment based records of precipitation variability in Guatemala along with a synthesis of Central American hydroclimate records spanning the last millennium (800–2000 CE). The synthesis reveals that regional climate changes have been strikingly heterogeneous, even over relatively short distances. Our analysis further suggests that shifts in the mean position of the Intertropical Convergence Zone, which have been invoked by numerous studies to explain variability in Central American and circum-Caribbean proxy records, cannot alone explain the observed pattern of hydroclimate variability. Instead, interactions between several ocean-atmosphere processes and their disparate influences across variable topography appear to have resulted in complex precipitation responses. These complexities highlight the difficulty of reconstructing past precipitation changes across Central America and point to the need for additional paleo-record development and analysis before the relationships between external forcing and hydroclimate change can be robustly determined. Such efforts should help anchor model-based predictions of future responses to continued global warming.

Plain Language Summary During the last 40 years, precipitation across much of Central America has decreased, creating problems for a region that depends heavily on rainfall for agriculture. Observations suggest, however, that precipitation changes are spatially complex with large differences over relatively short distances. This differs from climate model projections that indicate uniform drying for the entire Central American region. Using precipitation records derived from sediment and speleothems, we set out to explore whether over the past millennium Central American hydroclimate was characterized by relatively uniform changes across the region or if more complex patterns of hydroclimate change occurred. We acquired two new hydroclimate records from lakes in Guatemala and compare them with existing records from Central America. Our analysis indicates that precipitation has been highly variable across space and time and suggests that complex spatiotemporal patterns of precipitation variability in response to external forcing should be expected in the region.

1. Introduction

The last 40 years of Central American (CAM) hydroclimate have been marked by substantial complexity, including a decrease in precipitation in some locations and a general trend toward drier conditions (Stewart et al., 2021). This finding is especially alarming given that across much of the CAM region people rely heavily on agriculture for subsistence and are therefore vulnerable to prolonged drought. Precipitation regimes in the region are influenced by changes in the Intertropical Convergence Zone (ITCZ), the eastern tropical Pacific sea-surface temperatures (SSTs), the strength of the Caribbean Low Level Jet (CLLJ), the westward expansion of the North Atlantic Subtropical High (NASH) (Anderson et al., 2019; Martinez et al., 2019) and steep topographic gradients (Waylen et al., 1996; Imbach et al., 2018). Continued global warming will further influence moisture availability in the region (Almazroui et al., 2021; Neelin et al., 2006), potentially through changes in the width, strength and/or position of the ITCZ (Byrne & Schneider, 2016; Mamalakis et al., 2021). Limitations in regional instrumental data, however, have prevented the robust characterization of precipitation changes in many areas of Central America (Anderson et al., 2019; Stewart et al., 2021). For example, comparison of reanalysis and satellite-based

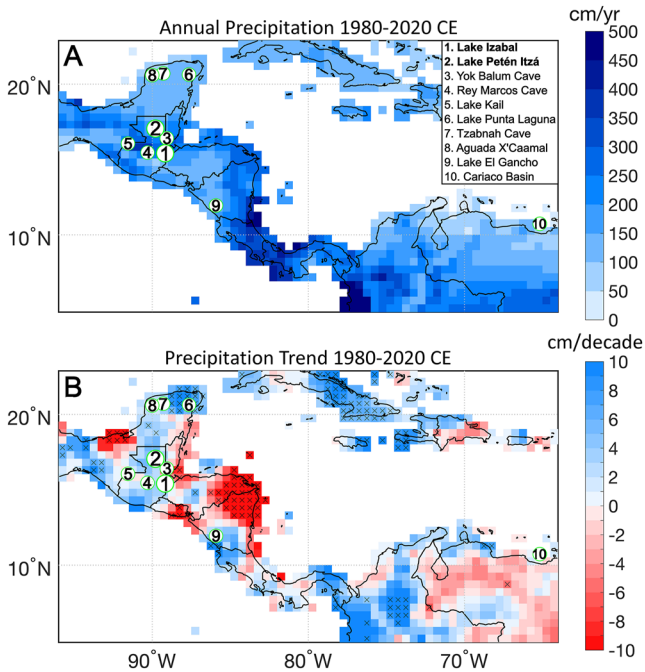

Figure 1. (a) Map of Central America, the Caribbean, and northern South America showing mean annual precipitation based on the Global Precipitation Climatology Center gridded data product (Schneider et al., 2011) spanning the period 1980–2020 CE. Green circles show the location of proxy records mentioned in the text. (b) Map showing the mean rate of change in annual precipitation (per decade). Rate of change is the slope of the linear trendline through the data at each grid cell. Black hatches denote cells for which the trend is significant at the $p < 0.1$ level. Note the large gradients in rate of change and mean precipitation in western Central America, especially in the region where substantial spatial heterogeneity is observed in the proxy records.

global climate data highlights significant differences between the datasets (Stewart et al., 2021), with distinct discrepancies in the rate of precipitation change in northern South America, Nicaragua, Honduras, El Salvador, and western Guatemala (Figure 1, Figure S1 in Supporting Information S1). These differences hinder assessments of climate model hindcasting of precipitation (Imbach et al., 2018). In addition, simulations of future hydroclimate patterns exhibit significant inter-model heterogeneities and fail to replicate the spatially complex precipitation patterns of present day (Bhattacharya & Coats, 2020; Christensen et al., 2007; Figure 1, Figure S2 in Supporting Information S1). Paleoclimate proxy evidence from Central America is therefore necessary for establishing a long-term perspective on hydroclimate variability that can inform model hindcasting and future projections.

One potential way to improve climate model projections is to focus on key periods in the recent past to contextualize observed changes in hydroclimate. A substantial body of evidence points to a change in ITCZ dynamics during the last millennium. This is especially true during the Little Ice Age (LIA; ~1300 to 1850 CE), when the ITCZ is hypothesized to have shifted to a more southerly mean position (Haug et al., 2001; Hodell et al., 2005; Steinman et al., 2022). Such an occurrence, were it to be conclusively identified in the paleo-proxy data, would provide insight on CAM hydroclimate responses to a potential future southward shift in the ITCZ, which some models project should occur as temperatures increase globally (Christensen et al., 2007; Mamalakis et al., 2021). Hydroclimate proxy evidence from CAM during the LIA, however, suggests significant heterogeneity, pointing to substantial spatial variability in hydroclimate. For example, proxy records from the northern Yucatán Peninsula (Hodell et al., 2005) and northern South America (Haug et al., 2001) indicate regional droughts at this time, suggesting a potential southward displacement of the rain belt, while proxy records from Belize (Asmerom et al., 2020), the highland regions of Guatemala (Stansell et al., 2020; Winter et al., 2020), central (Lozano-García et al., 2007) and northeastern Mexico (Wright et al., 2022), and El Salvador (Wojewódka-Przybył et al., 2022) do not support this pattern. This implies that ITCZ dynamics alone cannot explain the complex variability in CAM hydroclimate deduced from proxy records (Steinman et al., 2022). These contrasting results suggest that spatial heterogeneity in precipitation variability could be a persistent feature of CAM climate on decadal and longer timescales.

Here we present results from radiocarbon-dated sediment cores obtained from two lakes in the Guatemalan lowlands, Lake Petén Itzá (LPI core) and Lake Izabal (LI core). Our results, combined with a synthesis of proxy records from western CAM, show evidence of spatially complex patterns of hydroclimate change during the last millennium, especially during the LIA. Our analysis suggests that the development of additional paleoclimate records is needed to achieve clarity on how precipitation patterns have varied in CAM in response to external forcing and synoptic-scale circulation changes.

2. Study Area and Modern Climatology

Modern precipitation in CAM is influenced by the NASH, the ITCZ, the CLLJ, and changes in SSTs in both the Pacific and Atlantic basins (Martinez et al., 2019; Wright et al., 2022; Figure 2). The interaction of these ocean-atmosphere processes along with large topographic gradients (i.e., mountain ranges) produces complex spatial patterns of precipitation variability (Figure 1). For example, due to the high topography along the Caribbean coast of CAM, the CLLJ promotes orographic uplift, increasing precipitation in the area (Figure 1). During the summer, easterly winds bifurcate in the western Caribbean Sea, delivering moisture to the Yucatán Peninsula (Wang, 2007). During the winter, easterly winds shift southward away from the Yucatán Peninsula and across the CAM Isthmus toward the Pacific Ocean, reducing precipitation in the Yucatán, while increasing precipitation in the highland region of Guatemala through orographic effects (Martinez et al., 2019; Figure S2 in Supporting

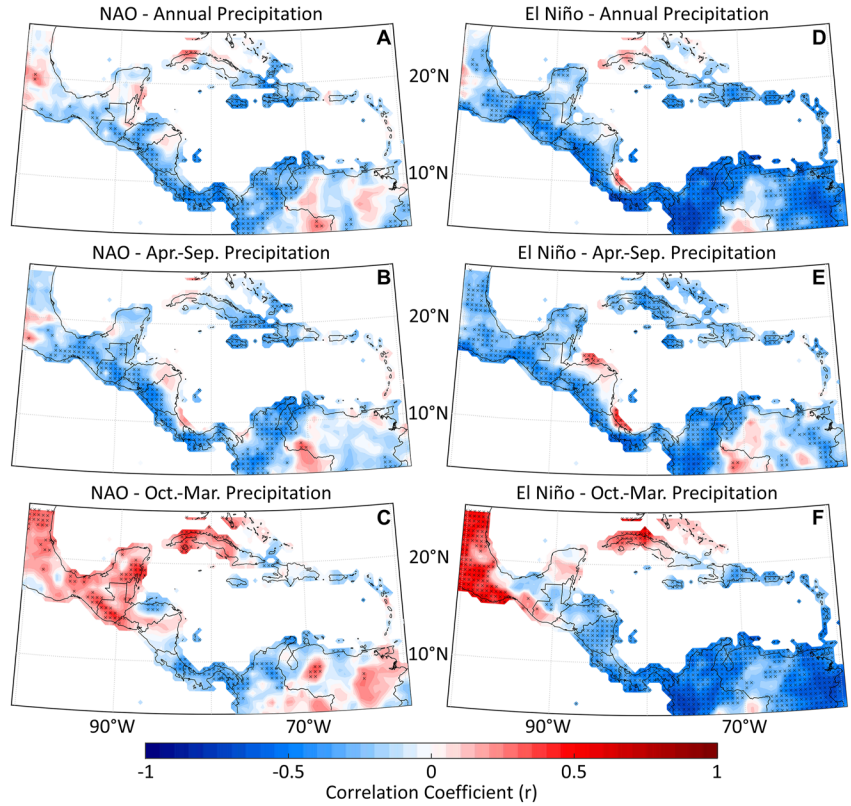

Figure 2. Correlation maps of annual (a and d), April to September (b and e), and October to March (c and f) precipitation amounts and climate indexes including NAO (a–c) and Niño3 SSTs (d–f). Precipitation data are based on the Global Precipitation Climatology Center gridded data product spanning 1980–2020 CE (Schneider et al., 2011). Black hatches mark regions of significance ($p < 0.1$). Scale bar depicts Pearson's r values.

Information S1). Disparities between the influence of the ITCZ, the CLLJ, the eastern tropical Pacific SSTs during El Niño Southern Oscillation (ENSO) events, and variations in the western extent of the NASH during positive North Atlantic Oscillation (NAO) events, combined with topographic complexities, has resulted in different rates of precipitation change across CAM during the last 40 years (Figures 1 and 2).

Lake Petén Itzá is located in northern Guatemala (Figure 1), having a surface area of 100 km^2, an elevation of ∼110 m above mean sea level, and a maximum depth of 160 m. The lake water is dominated by bicarbonate and sulfate, calcium, and magnesium ions (Hodell et al., 2008) with minimal river input. Lake Izabal is in the eastern lowlands of Guatemala at ∼1.5 m above mean sea level, with a surface area of 672 km^2 and a maximum depth of 15 m. Lake Izabal contains fresh water (Brinson & Nordlie, 1975), and riverine input is significant due to its large catchment (8,740 km^2; Obrist-Farner et al., 2019). Variations and interactions between the aforementioned ocean-atmosphere processes results in differing precipitation amounts at Izabal and Petén Itzá, with the former receiving around twice as much (∼3,300 vs. ∼1,800 mm yr^{-1}; Duarte et al., 2021).

3. Materials and Methods

3.1. Coring

Sediment cores were collected using two piston corers, one for unconsolidated mud-water interface (MWI) sediments (Fisher et al., 1992) and the other, a modified Livingstone corer, for deeper, consolidated sediments (Deevey, 1965). The cores were collected during two field seasons using a wooden platform mounted on two canoes. We collected two sediment cores, one from Lake Petén Itzá (LPI core; 515 cm long) and one from Lake Izabal (LI core; 455 cm long; Figure 1). In Petén Itzá (16°56′, 89°55′), the MWI core was collected to a sediment depth of 72 cm in 8.4 m of water. The core was extruded in the field at 2.0-cm intervals, and samples were placed in Whirl-Pak® bags. Six Livingstone core sections were retrieved, to a depth of 515 cm. In Izabal (15°24′,

89°16′), the MWI core was collected from the side of the platform to a sediment depth of 55 cm in 5.7 m of water. The core was extruded in the field at 3.0-cm intervals, and samples were placed in Whirl-Pak® bags. Four Livingstone core sections were retrieved, to a depth of 455 cm. Sediment cores were kept inside the polycarbonate core barrels and transported to Missouri University of Science and Technology for further analysis.

3.2. Radiocarbon Dating

We obtained accelerator mass spectrometry (AMS) radiocarbon dates from both cores using charcoal and terrestrial wood fragments. Samples were washed using deionized water and submitted to the Center for Accelerator Mass Spectrometry at Lawrence Livermore National Laboratory and to the National Ocean Sciences Accelerator Mass Spectrometry (NOSAMS) Facility at Woods Hole Oceanographic Institution. Samples were first treated with a standard acid-base-acid treatment, graphitized, and their radiocarbon concentrations measured via Accelerator Mass Spectrometry. Radiocarbon results were calibrated with OxCal 4.4 (Bronk Ramsey, 2009) using IntCal20 (Reimer et al., 2020). We established age-depth models with the Bayesian software Bacon (Blaauw & Christen, 2011) for the LPI and LI cores (Figures S3 and S4 in Supporting Information S1) using five and seven radiocarbon dates, respectively (Tables S1 and S2).

3.3. Core Scans and Photographs

Cores were scanned using a GEOTEK Multi-sensor core logger at the University of Florida and at the Continental Scientific Drilling Facility at the University of Minnesota. Cores were first scanned for magnetic susceptibility and density and then opened and split in half to obtain line-scan photographs. Sedimentological observations for both cores were carried out on split core surfaces with the aid of the line-scan photographs (Schnurrenberger et al., 2003). Bed color, sedimentary texture and structure, as well as bedding planes were observed and recorded at 1-cm intervals.

The split cores from both locations were analyzed at the Large Lakes Observatory, University of Minnesota, Duluth, USA, using an ITRAX XRF core scanner using a Cr source tube at 30 kV and 55 mA at 5-mm resolution with a 15-s dwell time (Figures S5 and S6 in Supporting Information S1). Raw data were reprocessed to optimize peak-fitting, using QSpec 8.6.0 software (Tables S3 and S4). We performed principal component analysis (PCA) in ©MATLAB to investigate the relationship between elements. Before PCA analysis, all elemental counts were standardized (converted to z-scores) to avoid confounding effects of dimensional heterogeneity. We utilized the combination of elemental abundances, elemental ratios, and PCA analysis to infer changes in lake catchment and in-lake processes (Figure S7 in Supporting Information S1). Elemental ratios discussed in the text are presented on a logarithmic scale due to the asymmetry associated with ratios (Figure S7 in Supporting Information S1). Finally, we did not carry out XRF analyses on the upper 50 cm of both cores due to the confounding effects of high-water content on XRF analysis (MacLachlan et al., 2015).

3.4. Proxy Data Age-Depth Modeling and Uncertainty Analysis

We analyzed eleven hydroclimate proxy records from lake sediment cores, marine sediment cores, and speleothems, and focused on 800 to 2000 CE. All proxy records were obtained from the NOAA/World Data Service for Paleoclimatology archives website (https://www.ncei.noaa.gov/access/paleo-search/). We focused on regional records that have published radiocarbon or U-Th ages, sufficient resolution for the correlation analysis, and cover the time interval of interest. For all eleven proxy records, we obtained the published radiocarbon (sediment cores) and U-Th (speleothems) dates and their uncertainties and utilized Bacon (Blaauw & Christen, 2011) to generate age-depth relationships (Figures S3, S4, S8–S16 in Supporting Information S1). Bacon (compiled in R) uses radiocarbon dates and other age-depth control points (e.g., date of core collection or U-Th dates) to model sedimentation rates for sediment cores and growth rates for speleothems and provides age uncertainty quantification. For all proxy sites, an additional date was introduced to constrain the most recent year of the record (i.e., the year of sample collection). For the radiocarbon-based age-depth models, we used IntCal20 (Reimer et al., 2020) to calibrate the dates. For the Cariaco Basin marine record, we used the published calibrated ages because the radiocarbon ages and the associated uncertainties were not available. For U-Th speleothem models, we used published calibrated U-Th ages and their uncertainties.

For the uncertainty analysis, 1000 age-depth pairs were obtained from Bacon, allowing us to generate 1000 age-proxy pairs for each record. We utilized the 1000 age-proxy pairs and resampled them at 5-year intervals

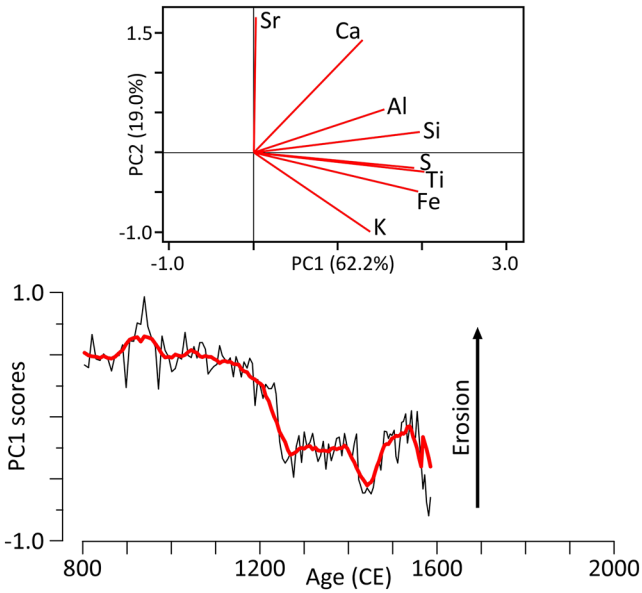

Figure 3. Principal component analysis for selected elemental abundances and time series data (black lines) and 10-point running mean (red lines) showing PC1 scores from Lake Petén Itzá. See Figures S5 and S7 in Supporting Information S1 for additional results.

using a linear interpolation. We used ©MATLAB to assemble age-model iterations for each proxy site, resulting in a range of proxy values for a specific modeled age (Figures S17–S27 in Supporting Information S1). We used the 1000 age-proxy pairs and calculated correlation coefficients and significance (p-values) and report the mean and 1σ for correlation values and the mean p-value (Figures S28 and S29 in Supporting Information S1). We used Bretherton's et al. (1999) formula for the effective sample size (ESS) given two time series X and Y (their Equation 30):

$$\mathrm{ESS} = N \frac{1}{\sum_{i=-(N-1)}^{(N-1)} \left(1 - \frac{|i|}{N}\right) \rho_i^X \rho_i^Y}$$

where N is the number of matching samples in both series, and the ρi's are the ith-lag autocorrelation coefficients of the individual time series. This is the more general expression of their Equation 31:

$$\mathrm{ESS} = N \frac{1 - \rho_1^X \rho_1^Y}{1 + \rho_1^X \rho_1^Y}$$

which is only valid when $\rho_1^X, \rho_1^Y \ll 1$.

4. Results and Interpretations

For both the LPI and LI cores, the ages of the terrestrial wood fragments are in stratigraphic order. The 515 cm-long LPI core covers the last ~7,000 years (Obrist-Farner & Rice, 2019; Figure S3 in Supporting Information S1, Table S1), while the 455 cm-long LI core is much shorter, covering the last ~1,400 years (Hernández et al., 2020; Figure S4 in Supporting Information S1, Table S2). Our results utilize the weighted mean modeled ages for both cores and are focused on the uppermost 50–115 cm (800–1585 CE) from the LPI core and between 55 and 435 cm (800–1926 CE) for the LI core.

4.1. Lake Petén Itzá

The LPI core segment of interest is characterized by thinly bedded carbonaceous mud that alternates in color between dark and light gray (Obrist-Farner & Rice, 2019). The mud contains variable amounts of gastropod shells and scattered organic debris. PCA analysis of elemental abundances shows that PC1 predominantly captures variability in terrigenous elements (Ti, Al, Fe, K, and Si). Titanium is relatively immobile and geochemically stable, and therefore its abundance in sedimentary systems is mainly attributed to upstream bedrock erosion and subsequent deposition in a sedimentary basin. The association of Al, Fe, K, and Si with Ti along PC1 (62.2% of the variance; Figure 3, Figure S5 in Supporting Information S1) suggests that changes in the abundance of these elements are likely indicative of changes in catchment erosion and runoff to the lake (e.g., Davies et al., 2015; Duarte et al., 2021; Kylander et al., 2011). Principal component 2 (19.0% of variance) explains variations related mostly to Sr and Ca (Figure 3) and reflects the presence of evaporites, potentially during times of low lake levels, reduced precipitation, and/or increased evaporation (e.g., Mueller et al., 2009; Kylander et al., 2011; Davies et al., 2015; Figure 3). We normalize Ca to Ti (Ca/Ti) to isolate the chemical Ca signal in the lake system as an additional proxy for increased evaporation (e.g., Davies et al., 2015; Kylander et al., 2011; Mueller et al., 2009; Figure S7 in Supporting Information S1).

From ~800 to ~1200 CE, elemental abundances from terrigenous elements (e.g., Ti, Al, and Si) decrease along with a slight decrease in PC1 scores (Figure S5 in Supporting Information S1, Table S3), indicating reduced catchment erosion for Lake Petén Itzá (Figure 3). During this time, there is a slight increase in Ca and S and in PC2 scores and in the log(Ca/Ti) values (Figure S7 in Supporting Information S1). After ~1200 CE, Ti, Al, Si, and K decrease and PC1 scores decline rapidly, while PC2 scores and the log(Ca/Ti) values exhibit a pronounced increase. These results suggest an increase in evaporation at Lake Petén Itzá that peaked at ~1320 CE. After ~1320 CE, terrigenous elemental abundance and PC1 scores remain low, and both PC2 scores and the log(Ca/Ti)

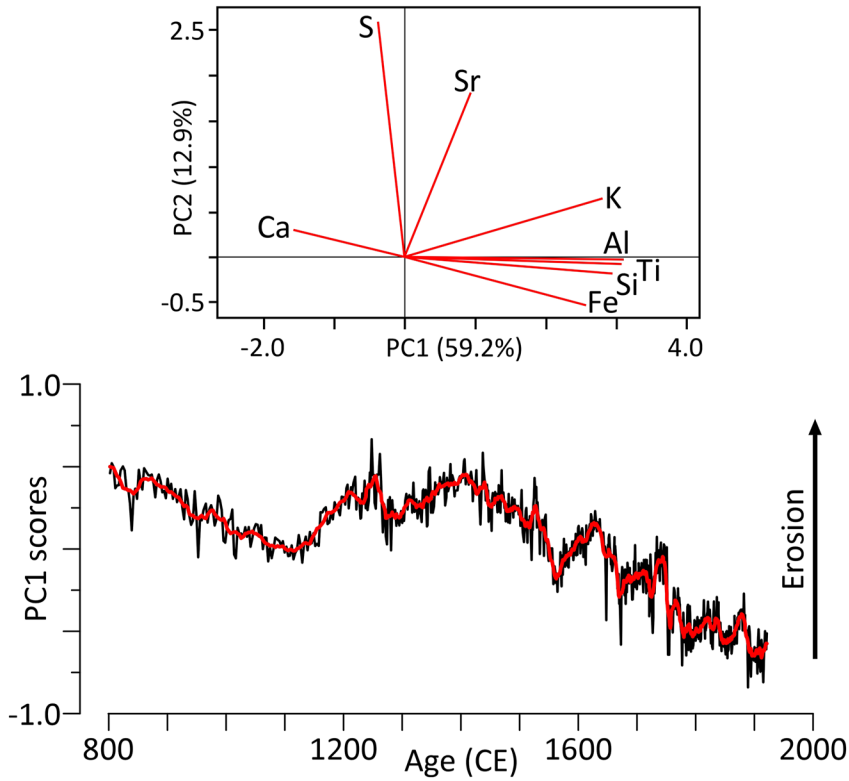

Figure 4. Principal component analysis for selected elemental abundances and time series data (black lines) and 10-point running mean (red lines) showing PC1 scores from Lake Petén Itzá. See Figures S6 and S7 in Supporting Information S1 for additional results.

values decrease toward the uppermost part of the interval, indicating continued low catchment erosion and a decrease in evaporation.

4.2. Lake Izabal

The LI core segment of interest is characterized by homogeneous olive gray silty mud that is faintly laminated and very thinly bedded with minimal organic debris (Hernández et al., 2020). The PCA results show that PC1 (59.2% of variance) mainly captures variability in Ti, Al, Si, Fe, and K (Figure 4, Figure S6 in Supporting Information S1). We infer that positive PC1 scores indicate an increase in catchment erosion and runoff (e.g., Davies et al., 2015; Duarte et al., 2021; Kylander et al., 2011; Figure 4), similar to the observations in the Petén core. Principal component 2 (12.9% of variance) for the LI core, however, mostly reflects changes in Sr and S. The processes that PC2 scores and the Ca and Ti ratio (Figure S7 in Supporting Information S1) reflect at Lake Izabal are ambiguous because S, Sr, and Ca in the lake can be related to evaporation, marine water transgression, or redox processes (Duarte et al., 2021; Obrist-Farner et al., 2022), and therefore are not used as indicators of hydroclimate in Izabal.

From ~800 to ~1140 CE, there is a decrease in both PC1 and terrigenous elemental abundances, such as Ti, Al, K, and Si (Figure 4, Figure S6 in Supporting Information S1, and Table S4) in the LI core. Similarly, there is an increase in the log(Ca/Ti) values and a slight decrease in PC2 scores (Figure S7 in Supporting Information S1). From ~1140 to ~1410 CE, there is an increase in PC1 scores and a decrease in the log(Ca/Ti) values, while PC2 scores are relatively constant through this interval (Figure S7 in Supporting Information S1). The PC1 results suggest a decrease in catchment erosion and runoff in the Lake Izabal area from ~800 to 1140 CE, followed by an increase from 1140 to 1410 CE. After ~1410 CE, PC1 scores decrease, supporting a decrease in catchment erosion and runoff. PC2 scores are highly variable after ~1410 CE with a minimum at ~1700 CE.

5. Discussion

There are at least two processes that could potentially explain the spatiotemporal variability in the proxy data from Petén Itzá and Izabal. First, changes in catchment erosion could have resulted from agricultural practices and deforestation in the catchments of both lakes. Paleolimnological investigations in Guatemala and the Yucatán Peninsula have shown a significant increase in catchment erosion during times of increased agricultural activities in the area, especially during the apogee of the Maya civilization (Brenner et al., 2002). Human settlements in the region were at their maximum extent at ~800 CE, resulting in significant erosion, as observed in sediment cores from many Petén lakes (Brenner et al., 2002). The collapse and disintegration of large cities led to rapid forest recovery (Curtis et al., 1998) with a coeval decrease in catchment erosion after ~1000 CE. Our Lake Petén Itzá record indicates a decrease in erosion in the area starting at ~1200 CE with a minimum in catchment erosion at ~1350 CE (95% range 1230–1420), while the Izabal record indicates an increase in erosion at ~1140 CE with a maximum occurring at ~1410 CE (95% range 1300–1440). These differences are difficult to reconcile by invoking changes in agricultural practices in the two watersheds. Our results, if explained solely by deforestation and agricultural practices, would suggest depopulation in the vicinity of Lake Petén Itzá and greater deforestation and agriculturally derived soil erosion around Izabal between 1300 and 1400 CE, an unlikely scenario given that population centers around Izabal were small and abandoned around 900 CE (Voorhies, 1972). Therefore, it is unlikely that the observed differences in the two records are principally due to human presence and agricultural practices.

A second possible mechanism for explaining the differences in the Petén Itzá and Izabal records is that the inferred changes in catchment erosion, as well as changes in evaporation at Lake Petén Itzá, resulted from different hydroclimate patterns at the two locations. For example, the decrease in erosion from 800 to ~1100 CE in both records could reflect a decrease in precipitation and increase in evaporation during the well-known Maya droughts (Hodell et al., 1995; Kennett et al., 2012). Between 800 and 1100 CE the two lake records are similar to other paleoclimate datasets from Guatemala, Belize, and the Yucatán Peninsula that suggest a decrease in precipitation at that time (e.g., Douglas et al., 2016). However, after this interval, the records diverge, with the Petén data indicating a decrease in erosion at ~1350 CE and the Izabal record showing a maximum in erosion at ~1410 CE. This difference suggests spatially complex hydroclimate in western CAM, especially after 1100 CE. One potential climate mechanism that could explain the difference observed between the Petén Itzá and Izabal records is a change in the intensity of the CLLJ along with topographic controls on moisture delivery to the region. Expansion of the western edge of the NASH could have resulted in a diversion of the CLLJ, the main source of moisture to the Petén region (Hastenrath, 1984). A southward shift in the CLLJ, combined with steep topography along the Caribbean coast, would have the potential to produce an increase in precipitation at Izabal through enhanced convergence via orographic uplift along with a reduction in precipitation at Petén Itzá. Alternatively, changes in Caribbean SSTs and the Atlantic Warm Pool could have resulted in an increase in moisture availability (e.g., Duarte et al., 2021; Winter et al., 2020) and through orographic uplift, greater precipitation along the Caribbean coast and central highlands of Guatemala.

Although these two mechanisms explain the differences observed in Petén and Izabal, additional CAM hydroclimate proxy records are highly heterogeneous even over relatively short distances, especially during the LIA (Figures 5 and 6). Notably, assessment of the relationship between proxy records in the region is made difficult by the uncertainties in radiocarbon and U-Th age-depth models and by the inherent differences in each of the proxy systems. For example, lakes of different sizes and degrees of hydrological closure should be expected to respond differently to changes in hydroclimate, and lake sediment archives from closed-basin settings will not capture the same information as speleothem isotope records, with the former reflecting the balance between evaporation and precipitation and the latter typically reflecting precipitation amount (e.g., Hodell et al., 1995; Lachniet, 2009). However, substantial disparities between the proxy records exist even when comparing only speleothem records (Figure S28 in Supporting Information S1), when comparing records from similar lacustrine systems (Figure S29 in Supporting Information S1), and when considering age-depth model uncertainties (Figures 5 and 6). For example, the YOK-G speleothem $\delta^{13}C$ record from Belize (Asmerom et al., 2020; ~70 km north from Izabal) is negatively correlated with Izabal ($r = -0.44 \pm 0.08$; Figure 6) and indicates wetter than average conditions from ~1400 to ~1850 CE, while both Izabal and the YOK-I speleothem $\delta^{18}O$ record (Kennett et al., 2012) are positively correlated ($r = 0.30 \pm 0.06$; Figure 6) and indicate peak precipitation at 1300–1410 CE and drier conditions thereafter (Figure 5). The Yok Balum records themselves exhibit a weak negative correlation ($r = -0.20 \pm 0.05$; Figure 6), indicating inconsistency in speleothem records from the same location. Additionally, the $\delta^{18}O$ record from Lake Kail in the western highlands (Stansell et al., 2020; ~250 km west from Izabal) and the Rey Marcos speleothem in the central highlands of Guatemala (Winter et al., 2020; ~100 km west from Izabal) do not exhibit significant correlations with Izabal or Petén Itzá (Figures 5 and 6) and

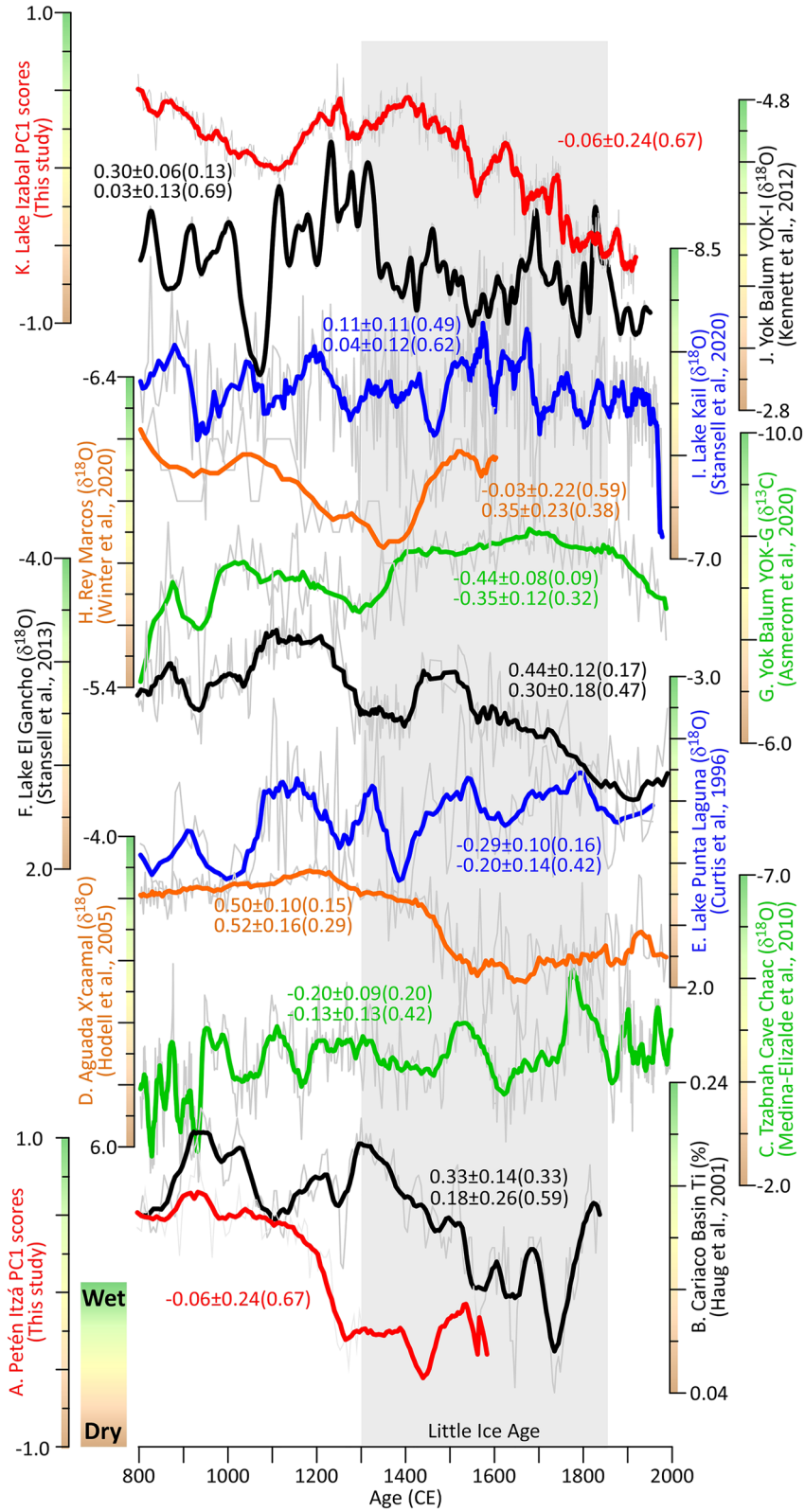

Figure 5. Proxy time series (gray lines) and 10-point running mean (colored lines) from (a) Lake Petén Itzá, (b) Cariaco Basin, (c) Chaac speleothem, (d) Aguada X'caamal, (e) Lake Punta Laguna, (f) Lake El Gancho, (g) Yok Balum YOK-G, (h) Rey Marcos, (i) Lake Kail, (j) Yok Balum YOK-I, and (k) Lake Izabal. Numbers show mean correlation coefficient values, 1σ, and *p*-values (see Figure 6) for the time series versus Izabal (upper numbers) and Petén Itzá (lower numbers).

10.1029/2022PA004445

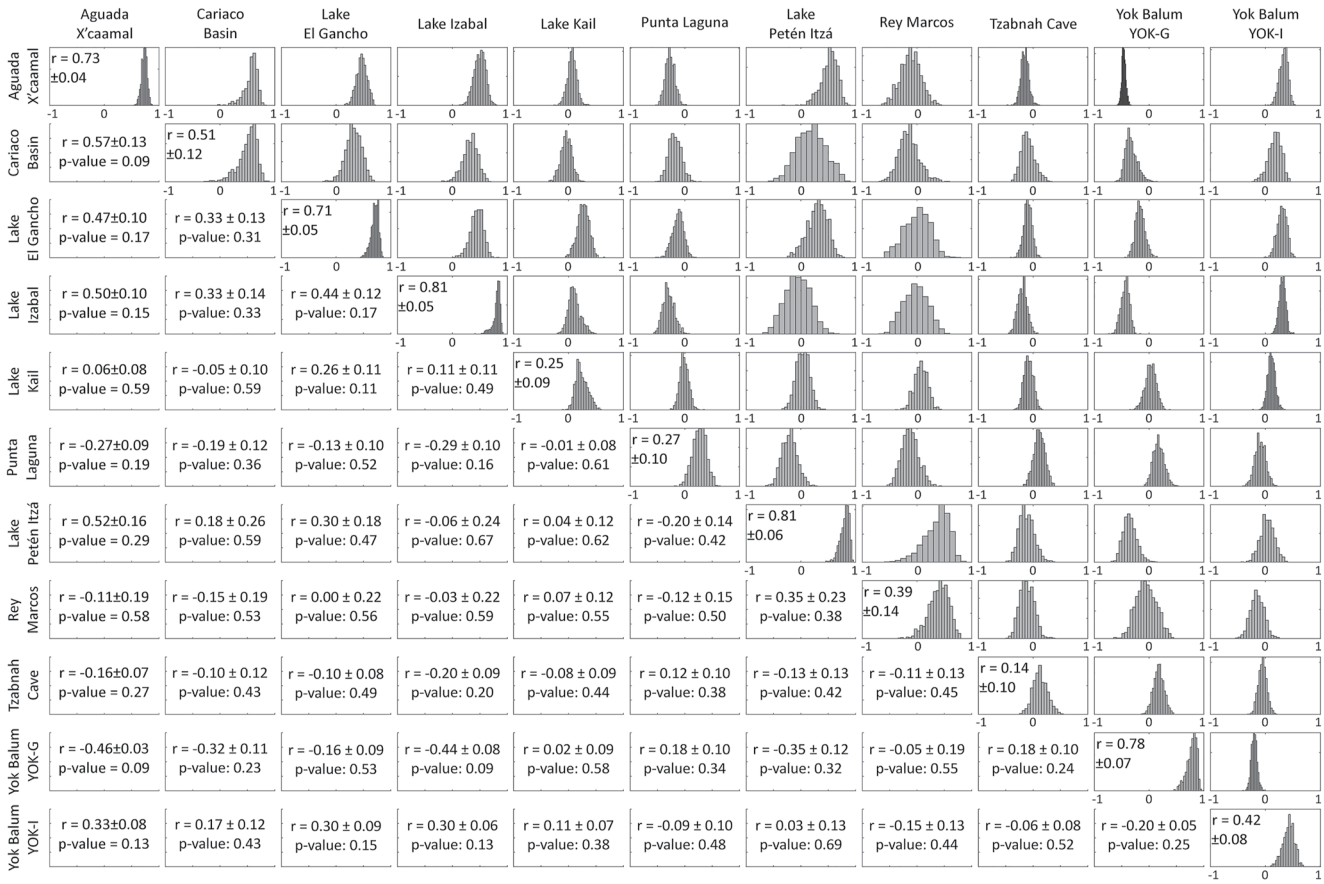

Figure 6. Matrix showing the range of correlation values (upper right) for all proxy record realizations utilizing 1000 age-proxy pairs (See Supporting Information S1). The diagonal quantifies the uncertainties in the age-depth model; for example, an age-depth model with no uncertainty would have correlation equal to 1. Each distribution represents how correlated each pair of sets of 1000 age-proxy realizations are to each other (see Supporting Information S1). The lower left shows mean correlation values, ±1σ, and mean *p*-values for the records analyzed. The $\delta^{18}O$ records have been multiplied by negative one so that positive correlation indicates consistent behavior between proxy sites.

indicate minimal change in precipitation and a reduction in precipitation at ~1350 CE, respectively. The $\delta^{18}O$ record from Lake Punta Laguna (Curtis et al., 1996) is negatively correlated with Izabal ($r = -0.29 \pm 0.10$) and Petén Itzá ($r = -0.20 \pm 0.14$; Figures 5 and 6) and indicates less precipitation between ~1150 and ~1400 CE and wetter conditions thereafter. In contrast, the Aguada X'caamal $\delta^{18}O$ record (Hodell et al., 2005; ~240 km west from Lake Punta Laguna) is positively correlated with Izabal ($r = 0.50 \pm 0.10$) and Petén Itzá ($r = 0.52 \pm 0.16$; Figures 5 and 6) and indicates persistently dry conditions after ~1250 CE. The Tzabnah Cave Chaac $\delta^{18}O$ record from the Yucatán Peninsula (Medina-Elizalde et al., 2010; ~40 km northeast from Aguada X'caamal) is negatively correlated with Izabal ($r = -0.20 \pm 0.09$) and Petén Itzá ($r = -0.13 \pm 0.13$) and indicates alternating dry and wet periods during the LIA.

Comparison between more distant records also supports our inference of profound hydroclimate heterogeneity in CAM. The $\delta^{18}O$ record from Lake El Gancho in Nicaragua (Stansell et al., 2013) is positively correlated with Izabal ($r = 0.44 \pm 0.12$; Figure 6) and Petén Itzá ($r = 0.30 \pm 0.18$; Figure 6) and indicates one short wet period between ~1400 and 1550 CE within an overall drying trend (Figures 5 and 6), similar to the observations from the Izabal and the YOK-I speleothem records. The onset of drying inferred from the Izabal record and the Cariaco Basin Ti record (Haug et al., 2001) are somewhat similar ($r = 0.33 \pm 0.14$; Figure 6); however, Petén Itzá indicates a reduction in precipitation at ~1350 CE, ~400 years earlier than the driest time in northern Venezuela (Figure 5). Interestingly, out of the 11 proxy records analyzed, only three of 55 cross-correlations are statistically significant ($p < 0.1$; Figures 5 and 6; see Supporting Information S1), highlighting the significant inconsistencies in the hydroclimate proxy records from CAM.

It is difficult to reconcile the distinct differences in hydroclimate proxy records from CAM by invoking changes in ITCZ dynamics alone. A southward shift in the ITCZ during the LIA (Haug et al., 2001; Hodell et al., 2005;

Steinman et al., 2022) would have produced persistent regional droughts in the CAM region during boreal summer if changes in the mean zonal position of the ITCZ were the only factor controlling hydroclimate. Our analysis does not support this inference, indicating that other ocean-atmosphere processes as well as local climate controls related to complex topography (e.g., Baldwin et al., 2021) must be stronger contributors than ITCZ dynamics to the complex hydroclimate changes observed in the CAM proxy records.

Asmerom et al. (2020) hypothesized that during the LIA, the ITCZ became wider and weaker, resulting in a decrease in precipitation in northern Venezuela and an increase along the northern flanks of the rain belt. However, the drying trend after the onset of the LIA inferred from Izabal and the YOK-I speleothem (Figure 6) suggests a more complex response to ocean-atmosphere forcing. A wider and weaker ITCZ during the LIA alone is insufficient to explain a drier Petén region at this time, as suggested by the proxy data from Lake Petén Itzá and Aguada X'caamal. An alternative hypothesis is that moisture availability in western CAM was affected by SST gradients between the Pacific and Atlantic oceans (Bhattacharya & Coats, 2020; Metcalfe et al., 2015) through changes in ENSO and NAO. Modern precipitation analysis indicates that positive ENSO events result in reduced precipitation across the entire Pacific coast of Central America (Dai & Wigley, 2000), whereas positive NAO conditions result in an increase in precipitation along the eastern coast of Guatemala, Belize, and the Yucatán Peninsula (Stansell et al., 2020; Figure 2). During the beginning of the last millennium, La Niña-like conditions (Cobb et al., 2003) and a more positive NAO (Mann et al., 2009) could have produced a wetter climate in both the Pacific coast of Central America and on the eastern coast of Guatemala, Belize, and the Yucatán Peninsula. In contrast, during the LIA, a change to El Niño-like conditions and a more negative NAO (Cobb et al., 2003; Mann et al., 2009) would have likely resulted in a drier climate across almost all of CAM. That the hydroclimate proxies do not express this pattern is potentially a result of there having been no century and longer timescale shift in NAO conditions over the last millennium and instead the development of short-lived, positive NAO phases in response to explosive volcanism (Ortega et al., 2015). Nevertheless, our proxy record synthesis indicates a regionally incoherent pattern of hydroclimate change during the last millennium, and especially during the LIA, that likely was not predominantly controlled by any one of these processes, and instead suggests that a variety of factors control hydroclimate patterns in CAM on multidecadal and longer timescales.

6. Conclusions

Our results highlight that interactions between numerous ocean-atmosphere processes, including the CLLJ, NAO, ENSO, and changes in ITCZ dynamics, as well as the effects of topography, make it difficult to understand external forcing impacts on hydroclimate in CAM. Modern-day precipitation patterns are also spatially complex, with large differences in precipitation amounts over short distances, especially along the mountain ranges and coasts of CAM. Available hydroclimate proxy data suggest that ITCZ dynamics (i.e., changes in latitudinal mean position, width and/or strength) alone are insufficient in explaining hydroclimate variability during the last millennium. Instead, the proxy data suggest that multiple ocean-atmosphere processes must have interacted to produce the inferred precipitation patterns across the northern tropical rainbelt. Additional proxy records from previously unexplored regions, such as the highland region and Pacific and Caribbean coasts of CAM could help clarify and disentangle the influence of external forcing and the various ocean-atmosphere circulation mechanisms on CAM hydroclimate. It would provide an enhanced basis of comparison for assessing the fidelity of data assimilation products and help with model-data comparisons to elucidate the various mechanisms influencing CAM hydroclimate.

Acknowledgments
The authors thank Oscar Nuñez, Heidy Garcia, Elmer Tun Pana, Noe Hernandez, and Defensores de la Naturaleza who provided lake access and helped us collect the sediment cores. The authors thank Anders Noren and Kristina Brady Shannon from the National Lacustrine Core Facility (LacCore) for help with core analyses and Robert Brown at the University of Minnesota-Duluth for help with XRF scanning. This study was supported by the National Science Foundation Grants EAR-2029102, EAR-1502989, and EAR-1502740. Lastly, the authors also thank three anonymous reviewers, the associate editor and editor Matthew Huber for insightful comments that helped improve the quality of our work.

Conflict of Interest

The authors declare no conflicts of interest relevant to this study.

Data Availability Statement

Data for replicating the results of this study are available at the National Oceanic and Atmospheric Administration National Centers for Environmental Information paleoclimate data repository (Obrist-Farner & Steinman, 2022).

References

Almazroui, M., Islam, M. N., Saeed, F., Saeed, S., Ismail, M., Ehsan, M. A., et al. (2021). Projected changes in temperature and precipitation over the United States, Central America, and the Caribbean in CMIP6 GCMs. *Earth Systems and Environment*, *5*(1), 1–24. https://doi.org/10.1007/s41748-021-00199-5

Anderson, T. G., Anchukaitis, K. J., Pons, D., & Taylor, M. (2019). Multiscale trends and precipitation extremes in the Central American midsummer drought. *Environmental Research Letters*, *14*(12), 124016. https://doi.org/10.1088/1748-9326/ab5023

Asmerom, Y., Baldini, J. U. L., Prufer, K. M., Polyak, V. J., Ridley, H. E., Aquino, V. V., et al. (2020). Intertropical convergence zone variability in the Neotropics during the common era. *Science Advances*, *6*(7), eaax3644. https://doi.org/10.1126/sciadv.aax3644

Baldwin, J. W., Atwood, A. R., Vecchi, G. A., & Battisti, D. S. (2021). Outsize influence of Central American orography on global climate. *AGU Advances*, *2*, e2020AV000343. https://doi.org/10.1029/2020AV000343

Bhattacharya, T., & Coats, S. (2020). Atlantic-Pacific gradients drive last millennium hydroclimate variability in Mesoamerica. *Geophysical Research Letters*, *47*(13), e2020GL088061. https://doi.org/10.1029/2020GL088061

Blaauw, M., & Christen, J. A. (2011). Flexible paleoclimate age-depth models using an autoregressive gamma process. *Bayesian Analysis*, *6*(3), 457–474. https://doi.org/10.1214/11-ba618

Brenner, M., Rosenmeier, M. F., Hodell, D. A., & Curtis, J. H. (2002). Paleolimnology of the Maya lowlands: Long-term perspectives on interactions among climate, environment, and humans. *Ancient Mesoamerica*, *13*(1), 141–157. https://doi.org/10.1017/s0956536102131063

Bretherton, C. S., Widmann, M., Dimnikov, V. P., Wallace, J. M., & Blade, I. (1999). The effective number of spatial degrees of freedom of a time-varying field. *Journal of Climate*, *12*(7), 1990–2009. https://doi.org/10.1175/1520-0442(1999)012<1990:TENOSD>2.0.CO;2

Brinson, M. M., & Nordlie, F. G. (1975). II. Lakes. 8. Central and South America: Lake Izabal, Guatemala. *SIL Proceedings, 1922-2010*, *19*(2), 1468–1479. https://doi.org/10.1080/03680770.1974.11896206

Bronk Ramsey, C. (2009). Bayesian analysis of radiocarbon dates. *Radiocarbon*, *51*(1), 337–360. https://doi.org/10.1017/s0033822200033865

Byrne, M. P., & Schneider, T. (2016). Narrowing of the ITCZ in a warming climate: Physical mechanisms. *Geophysical Research Letters*, *43*(21), 11350–11357. https://doi.org/10.1002/2016GL070396

Christensen, J. H., Hewitson, B., Busuioc, A., Chen, A., Gao, X., Held, I., et al. (2007). In *Regional climate projections*. Cambridge University Press.

Cobb, K. M., Charles, C. D., Cheng, H., & Edwards, R. L. (2003). El Niño/Southern Oscillation and tropical Pacific climate during the last millennium. *Nature*, *424*(6946), 271–276. https://doi.org/10.1038/nature01779

Curtis, J. H., Brenner, M., Hodell, D. A., Balser, R. A., Islebe, G. A., & Hooghiemstra, H. (1998). A multi-proxy study of Holocene environmental change in the Maya Lowlands of Peten, Guatemala. *Journal of Paleolimnology*, *19*(2), 139–159. https://doi.org/10.1023/A:1007968508262

Curtis, J. H., Hodell, D. A., & Brenner, M. (1996). Climate variability on the Yucatan Peninsula (Mexico) during the past 3500 years, and implications for Maya cultural evolution. *Quaternary Research*, *46*(1), 37–47. https://doi.org/10.1006/qres.1996.0042

Dai, A., & Wigley, T. M. L. (2000). Global patterns of ENSO-induced precipitation. *Geophysical Research Letters*, *27*(9), 1283–1286. https://doi.org/10.1029/1999GL011140

Davies, S. J., Lamb, H. F., & Roberts, S. J. (2015). Micro-XRF core scanning in palaeolimnology: Recent developments. In I. W. Croudace & R. G. Rothwell (Eds.), *Micro-XRF studies of sediment cores: Applications of a non-destructive tool for the environmental sciences* (pp. 189–226). Springer Netherlands.

Deevey, E. S. (1965). Sampling lake sediments by use of the Livingstone sampler. In B. Kummel & D. Raup (Eds.), *Handbook of paleontological techniques* (pp. 521–529). Freeman.

Douglas, P. M. J., Demarest, A. A., Brenner, M., & Canuto, M. A. (2016). Impacts of climate change and the collapse of lowland Maya civilization. *Annual Review of Earth and Planetary Sciences*, *44*(1), 613–645. https://doi.org/10.1146/annurev-earth-060115-012512

Duarte, E., Obrist-Farner, J., Correa-Metrio, A., & Steinman, B. A. (2021). A progressively wetter early through middle Holocene climate in the eastern lowlands of Guatemala. *Earth and Planetary Science Letters*, *561*, 116807. https://doi.org/10.1016/j.epsl.2021.116807

Fisher, M. M., Brenner, M., & Reddy, K. R. (1992). A simple, inexpensive piston corer for collecting undisturbed sediment/water interface profiles. *Journal of Paleolimnology*, *7*(2), 157–161. https://doi.org/10.1007/BF00196870

Hastenrath, S. (1984). Interannual variability and annual cycle: Mechanisms of circulation and climate in the tropical Atlantic sector. *Monthly Weather Review*, *112*(6), 1097–1107. https://doi.org/10.1175/1520-0493(1984)112%3C1097:IVAACM%3E2.0.CO;2

Haug, G. H., Hughen, K. A., Sigman, D. M., Peterson, L. C., & Röhl, U. (2001). Southward migration of the intertropical convergence zone through the Holocene. *Science*, *293*(5533), 1304–1308. https://doi.org/10.1126/science.1059725

Hernández, E., Obrist-Farner, J., Brenner, M., Kenney, W. F., Curtis, J. H., & Duarte, E. (2020). Natural and anthropogenic sources of lead, zinc, and nickel in sediments of Lake Izabal, Guatemala. *Journal of Environmental Sciences*, *96*, 117–126. https://doi.org/10.1016/j.jes.2020.04.020

Hodell, D. A., Anselmetti, F. S., Ariztegui, D., Brenner, M., Curtis, J. H., Gilli, A., et al. (2008). An 85-ka record of climate change in lowland Central America. *Quaternary Science Reviews*, *27*(11–12), 1152–1165. https://doi.org/10.1016/j.quascirev.2008.02.008

Hodell, D. A., Brenner, M., Curtis, J. H., Medina-González, R., Ildefonso-Chan Can, E., Albornaz-Pat, A., & Guilderson, T. P. (2005). Climate change on the Yucatan Peninsula during the Little Ice age. *Quaternary Research*, *63*(2), 109–121. https://doi.org/10.1016/j.yqres.2004.11.004

Hodell, D. A., Curtis, J. H., & Brenner, M. (1995). Possible role of climate in the collapse of Classic Maya civilization. *Nature*, *375*(6530), 391–394. https://doi.org/10.1038/375391a0

Imbach, P., Chou, S. C., Lyra, A., Rodrigues, D., Rodriguez, D., Latinovic, D., et al. (2018). Future climate change scenarios in Central America at high spatial resolution. *PLoS One*, *13*(4), e0193570. https://doi.org/10.1371/journal.pone.0193570

Kennett, D. J., Breitenbach, S. F. M., Aquino, V. V., Asmerom, Y., Awe, J., Baldini, J. U. L., et al. (2012). Development and disintegration of Maya political systems in response to climate change. *Science*, *338*(6108), 788–791. https://doi.org/10.1126/science.1226299

Kylander, M. E., Ampel, L., Wohlfarth, B., & Veres, D. (2011). High-resolution X-ray fluorescence core scanning analysis of Les Echets (France) sedimentary sequence: New insights from chemical proxies. *Journal of Quaternary Science*, *26*(1), 109–117. https://doi.org/10.1002/jqs.1438

Lachniet, M. S. (2009). Climatic and environmental controls on speleothem oxygen-isotope values. *Quaternary Science Reviews*, *28*(5), 412–432. https://doi.org/10.1016/j.quascirev.2008.10.021

Lozano-García, M. D. S., Caballero, M., Ortega, B., Rodríguez, A., & Sosa, S. (2007). Tracing the effects of the Little Ice age in the tropical lowlands of eastern Mesoamerica. *Proceedings of the National Academy of Sciences of the United States of America*, *104*(41), 16200–16203. https://doi.org/10.1073/pnas.0707896104

MacLachlan, S. E., Hunt, J. E., & Croudace, I. W. (2015). An empirical assessment of variable water content and grain-size on X-ray fluorescence core-scanning measurements of deep sea sediments. In I. W. Croudace & R. G. Rothwell (Eds.), *Micro-XRF studies of sediment cores: Applications of a non-destructive tool for the environmental sciences* (pp. 173–185). Springer Netherlands.

Mamalakis, A., Randerson, J. T., Yu, J.-Y., Pritchard, M. S., Magnusdottir, G., Smyth, P., et al. (2021). Zonally contrasting shifts of the tropical rain belt in response to climate change. *Nature Climate Change*, *11*(2), 143–151. https://doi.org/10.1038/s41558-020-00963-x

Mann, M. E., Zhang, Z., Rutherford, S., Bradley Raymond, S., Hughes Malcolm, K., Shindell, D., et al. (2009). Global signatures and dynamical origins of the little ice age and medieval climate anomaly. *Science*, *326*(5957), 1256–1260. https://doi.org/10.1126/science.1177303

Martinez, C., Goddard, L., Kushnir, Y., & Ting, M. (2019). Seasonal climatology and dynamical mechanisms of rainfall in the Caribbean. *Climate Dynamics*, *53*(1), 825–846. https://doi.org/10.1007/s00382-019-04616-4

Medina-Elizalde, M., Burns, S. J., Lea, D. W., Asmerom, Y., von Gunten, L., Polyak, V., et al. (2010). High resolution stalagmite climate record from the Yucatán Peninsula spanning the Maya terminal classic period. *Earth and Planetary Science Letters*, *298*(1), 255–262. https://doi.org/10.1016/j.epsl.2010.08.016

Metcalfe, S. E., Barron, J. A., & Davies, S. J. (2015). The Holocene history of the North American monsoon: "known knowns" and "known unknowns" in understanding its spatial and temporal complexity. *Quaternary Science Reviews*, *120*, 1–27. https://doi.org/10.1016/j.quascirev.2015.04.004

Mueller, A. D., Islebe, G. A., Hillesheim, M. B., Grzesik, D. A., Anselmetti, F. S., Ariztegui, D., et al. (2009). Climate drying and associated forest decline in the lowlands of northern Guatemala during the late Holocene. *Quaternary Research*, *71*(2), 133–141. https://doi.org/10.1016/j.yqres.2008.10.002

Neelin, J. D., Münnich, M., Su, H., Meyerson, J. E., & Holloway, C. E. (2006). Tropical drying trends in global warming models and observations. *Proceedings of the National Academy of Sciences of the United States of America*, *103*(16), 6110–6115. https://doi.org/10.1073/pnas.0601798103

Obrist-Farner, J., Brenner, M., Curtis, J. H., Kenney, W. F., & Salvinelli, C. (2019). Recent onset of eutrophication in Lake Izabal, the largest water body in Guatemala. *Journal of Paleolimnology*, *62*(4), 359–372. https://doi.org/10.1007/s10933-019-00091-3

Obrist-Farner, J., Brenner, M., Stone, J. R., Wojewódka-Przybył, M., Bauersachs, T., Eckert, A., et al. (2022). New estimates of the magnitude of the sea-level jump during the 8.2 ka event. *Geology*, *50*(1), 86–90. https://doi.org/10.1130/G49296.1

Obrist-Farner, J., & Rice, P. M. (2019). Nixtun-Ch'ich' and its environmental impact: Sedimentological and archaeological correlates in a core from Lake Petén Itzá in the southern Maya lowlands, Guatemala. *Journal of Archaeological Science: Report*, *26*, 101868. https://doi.org/10.1016/j.jasrep.2019.05.033

Obrist-Farner, J., & Steinman, B. A. (2022). NOAA/WDS Paleoclimatology—Lake sediment geochemical data from Guatemala [Dataset]. NOAA National Centers for Environmental Information. https://doi.org/10.25921/t2t7-ad71

Ortega, P., Lehner, F., Swingedouw, D., Masson-Delmotte, V., Raible, C. C., Casado, M., & Yiou, P. (2015). A model-tested North Atlantic Oscillation reconstruction for the past millennium. *Nature*, *523*(7558), 71–74. https://doi.org/10.1038/nature14518

Reimer, P. J., Austin, W. E. N., Bard, E., Bayliss, A., Blackwell, P. G., Bronk Ramsey, C., et al. (2020). The IntCal20 Northern Hemisphere radiocarbon age calibration curve (0–55 cal kBP). *Radiocarbon*, *62*(4), 725–757. https://doi.org/10.1017/RDC.2020.41

Schneider, U., Becker, A., Finger, P., Meyer-Christoffer, A., Rudolf, B., & Zeise, M. (2011). GPCC Full data reanalysis version 6.0 at 0.5°: Monthly land-surface precipitation from rain-gauges built on GTS-based and historic data. https://doi.org/10.5676/DWD_GPCC/FD_M_V6_050

Schnurrenberger, D., Russell, J., & Kelts, K. (2003). Classification of lacustrine sediments based on sedimentary components. *Journal of Paleolimnology*, *29*(2), 141–154. https://doi.org/10.1023/A:1023270324800

Stansell, N. D., Steinman, B. A., Lachniet, M. S., Feller, J., Harvey, W., Fernandez, A., et al. (2020). A lake sediment stable isotope record of late-middle to late Holocene hydroclimate variability in the Western Guatemala highlands. *Earth and Planetary Science Letters*, *542*, 116327. https://doi.org/10.1016/j.epsl.2020.116327

Stansell, N. D., Steinman, B. A., Abbott, M. B., Rubinov, M., & Roman-Lacayo, M. (2013). Lacustrine stable isotope record of precipitation changes in Nicaragua during the Little Ice age and medieval climate anomaly. *Geology*, *41*(2), 151–154. https://doi.org/10.1130/G33736.1

Steinman, B. A., Stansell, N. D., Mann, M. E., Cooke, C. A., Abbott, M. B., Vuille, M., et al. (2022). Interhemispheric antiphasing of neotropical precipitation during the past millennium. *Proceedings of the National Academy of Sciences of the United States of America*, *119*(17), e2120015119. https://doi.org/10.1073/pnas.2120015119

Stewart, I. T., Maurer, E. P., Stahl, K., & Joseph, K. (2021). Recent evidence for warmer and drier growing seasons in climate sensitive regions of Central America from multiple global datasets. *International Journal of Climatology*, *42*(3), 1399–1417. https://doi.org/10.1002/joc.7310

Voorhies, B. (1972). Settlement patterns in two regions of the southern Maya Lowlands. *American Antiquity*, *37*(1), 115–126. https://doi.org/10.2307/278893

Wang, C. (2007). Variability of the Caribbean low-level Jet and its relations to climate. *Climate Dynamics*, *29*(4), 411–422. https://doi.org/10.1007/s00382-007-0243-z

Waylen, P. R., Quesada, M. E., & Caviedes, C. N. (1996). Temporal and spatial variability of annual precipitation in Costa Rica and the Southern Oscillation. *International Journal of Climatology*, *16*(2), 173–193. https://doi.org/10.1002/(SICI)1097-0088(199602)16:2<173::AID-JOC12>3.0.CO;2-R

Winter, A., Zanchettin, D., Lachniet, M., Vieten, R., Pausata, F. S. R., Ljungqvist, F. C., et al. (2020). Initiation of a stable convective hydroclimatic regime in Central America circa 9000 years BP. *Nature Communications*, *11*(1), 716. https://doi.org/10.1038/s41467-020-14490-y

Wojewódka-Przybył, M., Krahn, K. J., Hamerlik, L., Macario-Gonzalez, L., Cohou, S., Charqueño-Celis, F., et al. (2022). Imprints of the Little Ice Age and the severe earthquake of AD 2001 on the aquatic ecosystem of a tropical maar lake in El Salvador. *The Holocene*, *32*(10), 1065–1080. https://doi.org/10.1177/09596836221106965

Wright, K. T., Johnson, K. R., Bhattacharya, T., Marks, G. S., McGee, D., Elsbury, D., et al. (2022). Precipitation in Northeast Mexico primarily controlled by the relative warming of Atlantic SSTs. *Geophysical Research Letters*, *49*(11), e2022GL098186. https://doi.org/10.1029/2022GL098186

References From the Supporting Information

Harris, I., Osborn, T. J., Jones, P., & Lister, D. (2020). Version 4 of the CRU TS monthly high-resolution gridded multivariate climate dataset. *Scientific Data*, *7*(1), 109. https://doi.org/10.1038/s41597-020-0453-3